

Enhanced exchange bias effects in a nanopatterned system consisting of two perpendicularly coupled ferromagnets

A. Bollero, B. Dieny, J. Sort, K. S. Buchanan, S. Landis, and J. Nogués

Citation: [Applied Physics Letters](#) **92**, 022508 (2008); doi: 10.1063/1.2833124

View online: <http://dx.doi.org/10.1063/1.2833124>

View Table of Contents: <http://scitation.aip.org/content/aip/journal/apl/92/2?ver=pdfcov>

Published by the [AIP Publishing](#)



Re-register for Table of Content Alerts

Create a profile.



Sign up today!



Enhanced exchange bias effects in a nanopatterned system consisting of two perpendicularly coupled ferromagnets

A. Bollero^{a)} and B. Dieny

SPINTEC (URA 2512 CNRS/CEA), CEA-Grenoble, 17 Av. Martyrs, 38054 Grenoble Cedex 9, France

J. Sort^{b)}

Institució Catalana de Recerca i Estudis Avançats (ICREA) and Departament de Física, Universitat Autònoma de Barcelona, 08193 Bellaterra, Barcelona, Spain

K. S. Buchanan

Center for Nanoscale Materials, Argonne National Laboratory, Argonne, Illinois 60439, USA

S. Landis

CEA-LETI Minatex, CEA Grenoble, 17 Av. Martyrs, 38054 Grenoble Cedex 9, France

J. Nogués

Institució Catalana de Recerca i Estudis Avançats (ICREA) and Institut Català de Nanotecnologia, Edifici CM7, Campus Universitat Autònoma de Barcelona, 08193 Bellaterra, Barcelona, Spain

(Received 13 September 2007; accepted 11 December 2007; published online 16 January 2008)

The effect of patterning on the shift of the hysteresis loop H_E and coercivity H_C in a system composed of two perpendicularly exchange-coupled ferromagnets (NiFe sputtered onto a [Pt/Co] multilayer) is investigated in long stripes and square dots. Setting the exchange bias coupling along the stripes results in a threefold increase of H_E compared to the continuous films. H_C increases dramatically when the coupling is set perpendicular to the stripes and also in the dots. Magnetic force microscopy studies and micromagnetic simulations suggest that differences in the number and orientation of the magnetic domains can account for the observed effects. © 2008 American Institute of Physics. [DOI: 10.1063/1.2833124]

Exchange-bias (EB) related phenomena result from interfacial exchange interactions usually between a ferromagnetic (FM) and an antiferromagnetic (AFM) material and it typically leads to a loop shift along the field axis, H_E .¹ Different models suggest that the magnetic domain structure of the AFM layer plays a fundamental role on the EB properties.^{2–5} Interestingly, opposite trends in H_E are found in the literature when comparing unpatterned with nanostructured exchange biased systems.^{6–11} The heating-cooling procedure often used to induce H_E can lead to undesirable structural effects (e.g., interdiffusion), which may in turn modify the magnetic behavior of the system. This has motivated the investigation of other types of systems and procedures.^{7,12–17} Recently, a novel approach for field-induced EB, based on multilayer structures consisting of two exchange coupled FM materials with mutually orthogonal easy axes has been proposed, Permalloy, NiFe (Ni₈₁Fe₁₉), with in-plane anisotropy, deposited onto a [Pt/Co] multilayer (ML), with perpendicular-to-plane anisotropy.¹² The procedure consists in in-plane saturation of the whole system followed by recording of the in-plane hysteresis loop with a maximum applied field strong enough to saturate the NiFe layer but not the [Pt/Co] ML. Intuitively, a perpendicular coupling should not result in any EB, similar to what is observed in AFM based systems.¹⁸ However, in-plane saturation of the system results in the creation of Néel-type flux closure caps in the [Pt/Co] ML with unequal sizes, i.e., enlarged domains parallel to the saturation direction.¹⁹ The coupling between the

NiFe magnetic moments and those of the [Pt/Co] ML through the top flux closure caps generated at the interface provides the bias.

In this letter, we study the effect of reducing the lateral size (i.e., patterning) on the loop shift and coercivity of a [Pt/Co]–NiFe system.

Si wafers were prepatterned by e-beam lithography and reactive ion etching to form 1×1 mm² arrays of Si stripes with lateral sizes of $200 \text{ nm} \times 1 \text{ mm}$, height of 200 nm, and spacing between stripes (trenches) of 200 nm. The inset of Fig. 1(a) shows a detail of this array. Square dots with lateral sizes, height, and periodicity of 200 nm were also prepared on identical Si wafers. Pt_{20 nm}/ [Co_{0.6 nm}/Pt_{1.8 nm}]₆/Co_{0.2 nm}/NiFe_{2.5 nm}/Cu_{2 nm}/Pt_{2 nm} ([Pt/Co]–NiFe) ML were dc-magnetron sputtered on the prepatterned wafers thereby coating the patterned stripes (or dots) and the trenches between them.

The loop shift H_E was induced by applying an in-plane magnetic field $H_0 = 11$ kOe and subsequently measuring the in-plane hysteresis loop, at room temperature, with a smaller maximum applied field, $H_{\text{hyst,max}}$, ranging from 1.5 to 4.25 kOe (sufficient to saturate the NiFe layer but not the [Pt/Co] ML), by longitudinal magneto-optical-Kerr effect (MOKE). The magnetic domain structures in the remanent state were imaged by magnetic force microscopy (MFM) with a low magnetic moment tip.²⁰ Micromagnetic simulations were carried out using a Landau-Lifshitz-Gilbert micromagnetic solver.²¹ The [Pt/Co]–NiFe system was considered as a NiFe layer exchange-coupled to a [Pt/Co] ML structure represented in three layers. Lateral dimensions of 200×1200 and 200×200 nm² were used for the stripes and the dots, respectively (see Ref. 22 for further details).

^{a)}Present address: Department of Energy, CIEMAT, Avda Complutense 22, 28040 Madrid, Spain. Electronic mail: alberto_bollero@yahoo.es.

^{b)}Electronic mail: jordi.sort@uab.es.

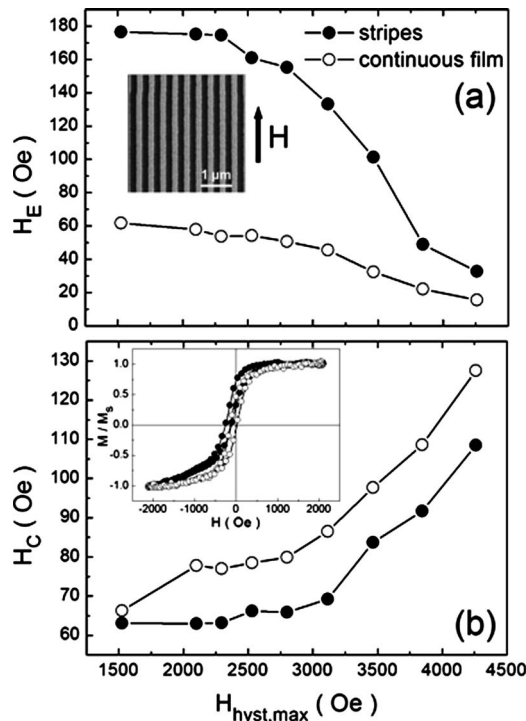


FIG. 1. Evolution of (a) the exchange bias field H_E and (b) the coercivity H_C with the maximum in-plane field $H_{\text{hyst,max}}$ after applying H_0 along the stripes (full symbols) and the continuous film (empty symbols). Also shown are a SEM image showing a detail of the array of stripes (upper inset), and hysteresis loops for both the stripes and the continuous film (bottom inset).

Figures 1(a) and 1(b) show the dependence of H_E and the coercivity H_C , respectively, on the maximum field $H_{\text{hyst,max}}$ applied along the stripes. Representative hysteresis loops for the case $H_{\text{hyst,max}} = 2100$ Oe are shown in the inset of Fig. 1(b). For low $H_{\text{hyst,max}}$ values the bias field in the stripes ($H_E \approx 180$ Oe) is much larger than for the continuous film ($H_E \approx 60$ Oe), in contrast to what is usually observed in patterned conventional EB systems.⁷ The values of H_E and H_C remain approximately constant for $H_{\text{hyst,max}} < 2500$ Oe both in the stripes and the continuous film. The observed decrease (increase) of H_E (H_C) with $H_{\text{hyst,max}}$ can be understood considering the progressive dragging of the net in-plane magnetic moment of the [Pt/Co] ML and the extra energy required to switch the in-plane magnetic moment arising from the [Pt/Co] ML.¹² The H_E values experience a more pronounced drop for the nanostructures than for the continuous part of the film for $H_{\text{hyst,max}} > 2500$ Oe which might be due to the more weakly coordinated spins located at the edges of the top of the stripes.⁶ For large enough $H_{\text{hyst,max}}$ values, the moments in the [Pt/Co] closure domains will reverse with the applied field, resulting in a zero net in-plane magnetic moment (i.e., no uncompensated spins), consequently the loop shift will vanish, as observed in Fig. 1(a).

To understand the difference in the H_E values between the stripes and the continuous films and bearing in mind that magnetic domains play a crucial role in EB,^{3,7,23,24} MFM images at remanence were recorded, after applying H_0 , for the continuous films [Fig. 2(a)] and the stripes (H_0 parallel to the stripes) [Fig. 2(b)]. Magnetic signal is measured from both the top of the nanostructures and the trenches between them since the deposition is carried out on prepatterned Si substrates. Note that these images mainly show the magnetic contrast stemming from the stripe domains in the [Pt/Co]

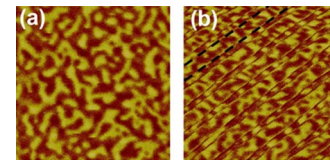


FIG. 2. (Color online) MFM images ($2.5 \times 2.5 \mu\text{m}^2$) at remanence after applying H_0 for (a) continuous film and (b) stripes (H_0 applied along them).

ML, which, in this system, play a role analogous to the AFM domains in AFM-FM bilayers. The magnetic domains are significantly reduced in the patterned structure.¹⁰ Since EB is due to the induced uncompensated moments, smaller domains (and the concomitant increase in the number of domain walls) lead to the enhanced H_E values in the patterned stripes compared to the continuous ML.^{7,23}

A drastically different behavior is observed in the case of applying H_0 and $H_{\text{hyst,max}}$ in-plane, perpendicular to the stripes. The corresponding hysteresis loop with $H_{\text{hyst,max}} = 3200$ Oe is shown in Fig. 3(a). Identical measurement procedure was applied to an array of 200 nm dots resulting in a similar hysteresis loop, as also shown in Fig. 3(a). In both cases, the loops exhibit a shift along the magnetic field axis and a dramatic enhancement of coercivity (from $H_C \approx 85$ Oe in the continuous film to $H_C > 1600$ Oe for the nanostructures). Note that both loops are very similar due to the identical dimension (200 nm) of the direction along which the external magnetic field is applied. The MFM images at remanence (after H_0) show that a wavy domain pattern tends to form in the stripes at remanence [Fig. 3(b)], while comparable magnetic configurations exhibiting a dipolar contrast indicative of a single flux closure cap state form in the square dots [Fig. 3(c)].

Additional insight into the understanding of the magnetic behavior of the system can be obtained from micro-magnetic simulations. Simulations of the stripes (Fig. 4) reveal that the magnetic configuration at remanence is constituted by fragmented domains orientated preferentially out of plane. The general character of the domain patterns after saturation parallel and perpendicular to the stripes is in good agreement with the MFM images shown in Figs. 2 and 3, respectively. The simulations also provide information of the evolution of the magnetic structure when following a complete hysteresis loop, as shown for the case $H_{\text{hyst,max}} = 3000$ Oe. The character of the PtCo domain configuration changes little as a function of field when measuring along the stripes [Fig. 4(a)] and, concomitantly, the simulated loop exhibits a pronounced shift along the magnetic field axis, of the

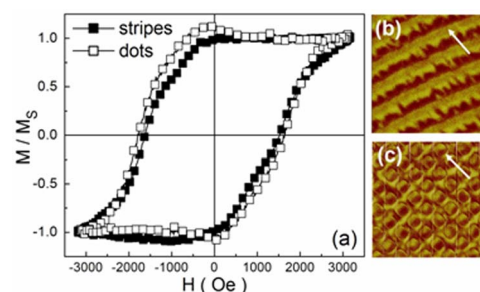


FIG. 3. (Color online) (a) In-plane hysteresis loops for the stripes (full symbols) and the dots (empty symbols) with both H_0 and $H_{\text{hyst,max}}$ applied perpendicular to the stripes. MFM images ($2.5 \times 2.5 \mu\text{m}^2$) at remanence after applying H_0 along the direction indicated by the white arrows for (b) stripes and (c) dots.

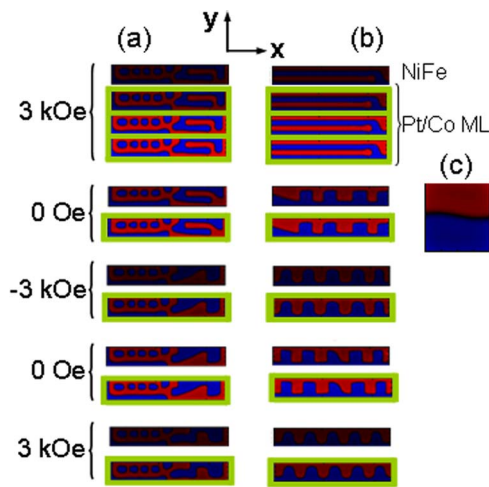


FIG. 4. (Color online) Two-dimensional magnetic configurations simulated for a stripe [(a), and (b)] and for a square dot, (c) when following a complete in-plane hysteresis loop with the field sequence along the x axis (a) and y axis, [(b) and (c)]. Blue and red indicate positive and negative out-of-plane magnetization, respectively. The magnetic configurations of the NiFe layer and all the Pt/Co bilayers are shown for $H=3$ kOe. Only the NiFe layer and the top PtCo layer are illustrated for all other fields.

same order of magnitude as in the loop measured experimentally (see Ref. 22). The simulation for the case of the stripes saturated and measured applying in-plane fields perpendicular to them [Fig. 4(b)], however, shows an evolution of the magnetization as a function of field. A multidomain configuration is displayed at $H_{\text{hyst,max}}$. Such magnetic structure sustained during magnetization reversal would be favourable to obtain an enlarged H_E . However, the simulations show a rapid transformation to a more stable dipolar configuration as the field is reduced that remains throughout the remainder of the hysteresis loop. The domain wall shape becomes wavy at remanence, with many domain walls parallel to the measurement direction, in excellent agreement with the MFM image [Fig. 3(b)]. Similar magnetic configuration is observed for the case of a simulated dot at remanence [Fig. 4(c)]. The simulations (see Ref. 22) suggest that the H_C enhancement results from rotation of the domain wall from being perpendicular to the applied field (at saturation) to being roughly parallel to the applied field direction (for $H \approx H_C$). Such partial rotation would occur so as to avoid having an energetically unfavourable flux closure domain pattern in the [Pt/Co] ML.

The simulated hysteresis loops,²² despite achieving only qualitative agreement with the experiment, due to the complexity of the system, showed a decrease in H_E with decreasing the number of domain walls perpendicular to the measuring direction. Domain walls oriented parallel to the field, in contrast, will have flux closure perpendicular to the measurement direction and contribute little to the exchange bias, being mainly responsible for the H_C enhancement. This result, coupled with the decreased domain size observed by MFM, supports the idea that the large H_E in these nanostructures in comparison to the continuous film is related to the increased ratio between uncompensated and compensated spins.

In conclusion, a large increase in the loop shift with respect to continuous films has been achieved for a nanostructured [Pt/Co]–NiFe system. As demonstrated by MFM studies, the domain sizes decrease upon patterning the system. This effect results in an increased ratio between uncompensated and compensated spins in the nanostructures which is responsible for the observed loop shift enhancement. Micromagnetic simulations have shown the key role played by the number of unequal closure domains, oriented perpendicular to the measuring field on increasing the loop shift.

Financial support from the 2005SGR-00401, the MAT-2007-66302-C02, and the HF2006-0197 research projects is acknowledged. A.B. acknowledges also support by the Spanish Ministry of Education and Science. Work at the Center for Nanoscale Materials was supported by the U. S. Department of Energy, Office of Science, Office of Basic Energy Sciences, under Contract No. DE-AC02-06CH11357.

- ¹J. Nogués and I. K. Schuller, *J. Magn. Magn. Mater.* **192**, 203 (1999); A. E. Berkowitz and K. Takano, *ibid.* **200**, 552 (1999); R. L. Stamps, *J. Phys. D* **33**, R247 (2000); M. Kiwi, *J. Magn. Magn. Mater.* **234**, 584 (2001).
- ²D. Mauri, H. C. Siegmann, P. S. Bagus, and E. Kay, *J. Appl. Phys.* **62**, 3047 (1987).
- ³A. P. Malozemoff, *Phys. Rev. B* **35**, 3679 (1987).
- ⁴N. C. Koon, *Phys. Rev. Lett.* **78**, 4865 (1997).
- ⁵U. Novak, K. D. Usadel, J. Keller, P. Miltenyi, B. Beschoten, and G. Güntherodt, *Phys. Rev. B* **66**, 014430 (2002).
- ⁶V. Baltz, J. Sort, S. Landis, B. Rodmacq, and B. Dieny, *Phys. Rev. Lett.* **94**, 117201 (2005).
- ⁷J. Nogués, J. Sort, V. Langlais, V. Skumryev, S. Suriñach, J. S. Muñoz, and M. D. Baró, *Phys. Rep.* **422**, 65 (2005).
- ⁸A. Nemoto, Y. Otani, S. G. Kim, K. Fukamichi, O. Kitakami, and Y. Shimada, *Appl. Phys. Lett.* **74**, 4026 (1999).
- ⁹Y.-J. Wang and C.-H. Lai, *J. Appl. Phys.* **89**, 7537 (2001).
- ¹⁰M. Fraune, U. Rüdiger, G. Güntherodt, S. Cardoso, and P. Freitas, *Appl. Phys. Lett.* **77**, 3815 (2000).
- ¹¹E. Girgis, R. D. Portugal, H. Loosvelt, M. J. Van Bael, I. Gordon, M. Malfait, K. Temst, C. Van Haesendonck, L. H. A. Leunissen, and R. Jonckheere, *Phys. Rev. Lett.* **91**, 187202 (2003).
- ¹²J. Sort, A. Popa, B. Rodmacq, and B. Dieny, *Phys. Rev. B* **70**, 174431 (2004).
- ¹³J. Torrejón, L. Kraus, K. R. Pirota, G. Badini, and M. Vázquez, *J. Appl. Phys.* **101**, 09N105 (2007).
- ¹⁴G. Gubbiotti, G. Carlotti, M. Madami, J. Weston, P. Vavassori, and G. Zangari, *IEEE Trans. Magn.* **38**, 2779 (2002).
- ¹⁵K. Dumesnil, M. Dutheil, C. Dufour, and Ph. Mangin, *Phys. Rev. B* **62**, 1136 (2000).
- ¹⁶M. Cheon, Z. Liu, and D. Lederman, *Appl. Phys. Lett.* **90**, 012511 (2007).
- ¹⁷S. Sahoo, T. Mukherjee, K. D. Belashchenko, and Ch. Binek, *Appl. Phys. Lett.* **91**, 172506 (2007).
- ¹⁸J. Nogués, T. J. Moran, D. Lederman, I. K. Schuller, and K. V. Rao, *Phys. Rev. B* **59**, 6984 (1999).
- ¹⁹A. Bollero, L. D. Buda-Prejbeanu, V. Baltz, J. Sort, B. Rodmacq, and B. Dieny, *Phys. Rev. B* **73**, 144407 (2006).
- ²⁰X. Zhu, P. Grütter, V. Metlushko, and B. Ilıc, *Phys. Rev. B* **66**, 024423 (2002).
- ²¹LLG Micromagnetics Simulator™, M. R. Scheinfein.
- ²²See EPAPS Document No. E-APPLAB-92-035803 for supplementary material that includes details about the micromagnetic simulations and simulated hysteresis loops of the nanostructured [Pt/Co]–NiFe system. This document can be reached through a direct link in the online article's HTML reference section or via the EPAPS homepage (<http://www.aip.org/pubservs/epaps.html>).
- ²³A. Scholl, F. Nolting, J. W. Seo, H. Ohldag, J. Stöhr, S. Raoux, J.-P. Locquet, and J. Fompeyrine, *Appl. Phys. Lett.* **85**, 4085 (2004).
- ²⁴C. Leighton, J. Nogués, B. J. Jönsson-Åkerman, and I. K. Schuller, *Phys. Rev. Lett.* **84**, 3466 (2000).